JOURNAL OF VIROLOGY, Feb. 2005, p. 1853–1860 Vol. 79, No. 3
0022-538X/05/$08.00+0 doi:10.1128/JVI.79.3.1853–1860.2005

Atypical Fusion Peptide of Nelson Bay Virus Fusion-Associated Small Transmembrane Protein

LiTing T. Cheng, Richard K. Plemper, and Richard W. Compans*

Department of Microbiology and Immunology, Emory University School of Medicine, Atlanta, Georgia

Received 5 May 2004/Accepted 19 September 2004

A 10-kDa nonstructural transmembrane protein (p10) encoded by a reovirus, Nelson Bay virus, has been shown to induce syncytium formation (34). Sequence analysis and structural studies identified p10 as a type I membrane protein with a central transmembrane domain, a cytoplasmic basic region, and an N-terminal hydrophobic domain (HD) that was hypothesized to function as a fusion peptide. We performed mutational analysis on this slightly hydrophobic motif to identify possible structural requirements for fusion activity. Bulky aliphatic residues were found to be essential for optimal fusion, and an aromatic or highly hydrophobic side chain was found to be required at position 12. The requirement for hydrophilic residues within the HD was also examined: substitution of 10-Ser or 14-Ser with hydrophobic residues was found to reduce cell surface expression of p10 and delayed the onset of syncytium formation. Nonconservative substitutions of charged residues in the HD did not have an effect on fusion activity. Taken together, our results suggest that the HD is involved in both syncytium formation and in determining p10 transport and surface expression.

Membrane fusion plays important roles in biological processes such as vesicular trafficking, myoblast differentiation, and virus entry (1, 3, 18, 20, 40). The mechanism of protein-mediated membrane fusion has been studied extensively with the surface glycoproteins of enveloped viruses. Based on structural differences, viral glycoproteins can be separated into class I and class II fusion proteins. Class I proteins, exemplified by the hemagglutinin (HA) protein of influenza virus (37, 41), form spikes that protrude from the viral surface and induce fusion through conformational changes (5). After a triggering event, either the lowering of pH (as for HA) or receptor binding, a coiled-coil structure is extended toward the target membrane. A highly hydrophobic domain (HD), the fusion peptide (7, 36), located at the membrane distal end of the coiled-coil structure is then inserted into the target membrane. Subsequent conformational changes, aided by the presence of two sets of heptad repeats within the coiled coil, allow the formation of a six-helix bundle structure and bring the two lipid membranes into close proximity for fusion. In contrast, class II fusion proteins (16, 33), such as the envelope protein of tick-borne encephalitis virus, are composed predominantly of β-sheets and lie parallel to the surface of the viruses. Rearrangements and reorientations of individual domains, along with the insertion of fusion peptides, are necessary for class II fusion (15).

Recent studies of fusogenic members of the *Orthoreovirus* genus have identified a new class of syncytium-inducing proteins termed fusion-associated small transmembrane (FAST) protein (34). Identified thus far in Nelson Bay virus (NBV), baboon reovirus (8), reptilian reovirus (6), and various avian reovirus (ARV) strains (12, 23, 28), FAST proteins are nonstructural, transmembrane proteins thought to aid in cell-to-cell spread by inducing syncytium formation (11). Because of their low molecular masses (ranging from 10 kDa to 15 kDa) and apparent lack of typical fusion protein motifs such as the heptad repeats, FAST proteins most likely cause fusion through a novel mechanism. Previous work on the FAST proteins (also termed p10 because of their molecular masses) of ARV and NBV determined that they are type I membrane proteins with a central transmembrane domain, a cytoplasmic basic region, and an N-terminal HD that was hypothesized to function as a fusion peptide (34).

To further investigate the fusion mechanism of NBVp10, we performed mutational analysis to examine the role of the slightly HD in fusion activity. Since most known fusion peptides are highly hydrophobic, we introduced conservative (A and L) and nonconservative (G and R) mutations at hydrophobic residues and assessed the effect of the mutations on syncytium formation and lipid mixing. The roles in fusion of hydrophilic and charged residues in the HD were also examined.

MATERIALS AND METHODS

Cells and virus. Monolayer cultures of Vero and rat XC cells were maintained in Dulbecco modified minimal essential medium supplemented with 10% fetal calf serum (HyClone Laboratories, Logan, Utah). Stocks of NBV (14) were grown in Vero cells.

NBV p10 antiserum production. Synthetic peptides corresponding to the ectodomain (the first 39 amino acids) and the cytoplasmic domain (the first 37 amino acids immediately after transmembrane domain) of NBV p10 were used to inject rabbits for antibody production (Rockland Immunochemicals, Gilbertsville, Pa.). A total of 10 mg of each peptide was conjugated with keyhole limpet hemocyanin. The rabbits (two rabbits per peptide) were then injected intradermally with 500 μg of the conjugated peptides, followed by four weekly boosts subcutaneously with 250 μg of the peptides. Only the rabbits injected with peptides corresponding to the cytoplasmic domain produced antibodies capable of detecting p10 in a Western blot analysis.

Cloning and chimeric PCR mutagenesis. Total RNA collected from NBV-infected cells was used to obtain a cDNA encoding p10 by reverse transcription-PCR. Flanking ClaI and SphI sites were introduced for cloning into the mammalian vector pCAGGS.MCS (29). Three-step chimeric PCR with two external primers and two nested primers containing the desired mutation was used to introduce point mutations. Furthermore, as previously done (34), we optimized the translation start site (from UCGAUAUG to CCACCAUG.) PCR products were then introduced into the pCAGGS vector, and the sequences of the inserts were confirmed.

* Corresponding author. Mailing address: Department of Microbiology and Immunology, Emory University School of Medicine, 1510 Clifton Rd., Rm. 3001, Atlanta, GA 30322. Phone: (404) 727-5947. Fax: (404) 727-8250. E-mail: compans@microbio.emory.edu.

Transfection, cell surface biotinylation, and Western blot analysis. A total of 0.75 μg of each plasmid encoding mutant p10 was transfected by using Lipofectamine 2000 (Invitrogen, Carlsbad, Calif.) into confluent Vero cells in 12-well plates, with each well containing 5×10^5 cells. At 18 h posttransfection, the cells were washed with phosphate-buffered saline before incubation with EZ-Link NHS-SS-biotin (Pierce, Rockford, Ill.) at 4°C. Then, 10% serum containing Dulbecco modified Eagle medium was used for quenching. The cells were then lysed with radioimmunoprecipitation assay buffer (50 mM Tris-HCl [pH 7.6], 150 mM NaCl, 0.5% Triton X-100, 0.5% sodium dodecyl sulfate [SDS], and protease inhibitor [Roche, Basel, Switzerland]). Avidin-agarose beads (Pierce) were used to purify the biotinylated surface proteins. Western blot analysis was performed on the surface and total cell lysate samples (both reduced and nonreduced) by using SDS–15% polyacrylamide gel electrophoresis. A 1:1,000 dilution of the rabbit anti-NBV p10 antibody was used. As internal controls, the Western blot membranes were reprobed with anti-human transferrin receptor antibody (Zymed, South San Francisco, Calif.). Quantitation of the chemiluminescent signals was performed with a digital imaging system (VersaDoc; Bio-Rad, Hercules, Calif.). Western blot membranes were exposed directly to the camera of the VersaDoc system, which captures a three-dimensional image and allows a volumetric determination of light signals.

Syncytium assay. First, 1 μg of each plasmid encoding mutant p10 was transfected into Vero cells, and the extent of cell-cell fusion was observed 24, 36, 48, and 72 h posttransfection under the light microscope. Then, the syncytia, defined as multinucleated cells with at least four nuclei, per microscope field at ×100 magnification were counted. Ten fields were selected at random and counted for each time point. The extent of fusion induced by the mutant p10 protein was classified into either no fusion (−) or one of four levels of syncytium formation—+, 1 to 25%; ++, 26 to 50%, +++, 51 to 75%, and ++++, 76 to 100%—by comparison to the wild-type p10 protein. The extent of fusion induced by wild-type p10 was designated "++++" (>80% of the surface area is covered by syncytial cells) at 24 h posttransfection. When the monolayer is destroyed by syncytium formation over time, the time point is designated "D" (for detached).

Dye transfer assay. XC cells were suspended in phosphate-buffered saline and doubly labeled with octadecyl rhodamine B (R18) and Calcein AM (both from Molecular Probes, Eugene, Oreg.) according to the manufacturer's instructions (2). Vero cells expressing mutant p10 were suspended and reseeded with labeled XC cells at a 1:1 ratio. Lipid and content mixing were observed at 4 h after reseeding.

RESULTS

Design and hydrophobicity plots of mutant NBV p10. To investigate the importance of the hydrophobic nature of the HD, the hydrophobic residues at positions 8-Ile, 9-Val, 11-Val, 12-Phe, or 15-Val (Fig. 1A) were changed to Ala, Gly, or Arg by chimeric PCR. In addition, aromatic residues Trp and Tyr were introduced at position 12 to assess the requirement for aromatic side chains. To investigate the role of hydrophilic residues at position 10-Ser and14-Ser, we introduced Ala and Val substitutions. Finally, we introduced Ala and Asp at position 16-His to determine the requirement for a charged residue in this region. The changes in hydrophobicity of the HD due to substitutions were predicted by using the Kyte and Doolittle plot (22). In general, the contribution of individual amino acids to the overall hydrophobicity can be ranked as follows: Val = Ile = Leu > Phe = Trp > Ala > Gly > Arg. Shown as an example in Fig. 1B is the decrease in hydrophobicity of the HD as we change 11-Val to Ala, Gly, or Arg. Plasmids encoding the mutant p10 proteins described above were transfected into Vero cells to assess their effects on syncytium formation.

Expression and cell surface localization of mutant NBV p10. Since the introduction of point mutations into NBV p10 can alter protein transport or processing, we determined the overall expression levels by using Western blot analysis and cell surface levels through surface biotinylation. Our results (Fig. 2) showed the general tendency that when hydrophobic residues were mutated to less hydrophobic amino acids, the overall and surface steady-state levels increased significantly compared to wild-type NBV p10. Mutant V11G, for example, showed a 6,200% increase in chemiluminescence signal at the surface and a 2,100% increase for overall expression level compared to the wild type (see Fig. 4). The differences in expression levels for other mutants are less pronounced but still significant, mostly between a three- and fivefold increase in chemiluminescence signals. The reduction in hydrophobicity appeared to increase the stability of p10, thus increasing the overall steady-state level. When conservative changes (to Leu) were introduced at these hydrophobic residues, we observed various surface expression levels (Fig. 3 and Fig. 4A). Since the differential in expression levels shown in Fig. 4 is so drastic, the Western blot membranes were reprobed for transferrin receptors as an internal control. The variations in the amount of transferrin receptors detected between samples were found to be within an acceptable range, from 12.8 to 17.9%. The quantitation data of the expression levels shown in Fig. 4 were the results of three separate experiments, with an average standard deviation of 36.5% (which is negligible in the context of 300 to 6,200% differentials observed).

Mutation of hydrophilic residues to hydrophobic residues (S10V and S14V) was found to reduce surface expression level at 24 h posttransfection (Fig. 3) (59.1% reduction compared to wild-type for S10V and 75.2% reduction for S14V as quantitated by VersaDoc imaging). However, as will be shown below, S10V and S14V mutants did cause syncytium formation at later time points, indicating that these mutant proteins can accumulate over time and retained their fusion ability. Mutations of charged residues (H16A and H16D) did not result in adverse effects on protein expression (Fig. 3). In general, the hydrophobicity of HD of NBV p10 is negatively correlated with the steady-state surface expression level, although hydrophobicity is also required for effective fusion.

Our results also suggest that NBV p10 homo-oligomerizes as shown by the presence of antigenic bands with estimated 20-kDa molecular mass when analyzed under nonreducing conditions (Fig. 2 and 3). When the total cell lysates were analyzed under reducing conditions, the potential dimers disappeared as expected, indicating the involvement of disulfide bonds in dimer formation. For most of the mutants examined, Western blot analysis showed that a similar proportion of each mutant p10 protein was found to form dimers.

Syncytium formation by p10 mutants with point mutations at hydrophobic residues. To determine the effects of point mutations at hydrophobic residues (8-Ile, 9-Val, 11-Val, 12-Phe, and 15-Val) on syncytium formation, cells were transfected with plasmids encoding mutant p10 proteins and observed over a period of 3 days posttransfection (Table 1). Wild-type NBV p10 induced extensive fusion at 24 h posttransfection (Fig. 4), and by day 2 the monolayer was destroyed. Mutations of the hydrophobic residues to Gly completely abolished fusion for the period observed, except at 9-Val where the fusion extent was reduced by half compared to the wild type. When the hydrophobic residues were changed to Ala, all positions except residue 12 retained fusion to various degrees. Mutation of the hydrophobic residues to the charged residue Arg was not well tolerated; only a small number of syncytia were observed for I8R and V9R mutants, whereas none were observed for V11R, V15R, and F12R. Conservative changes

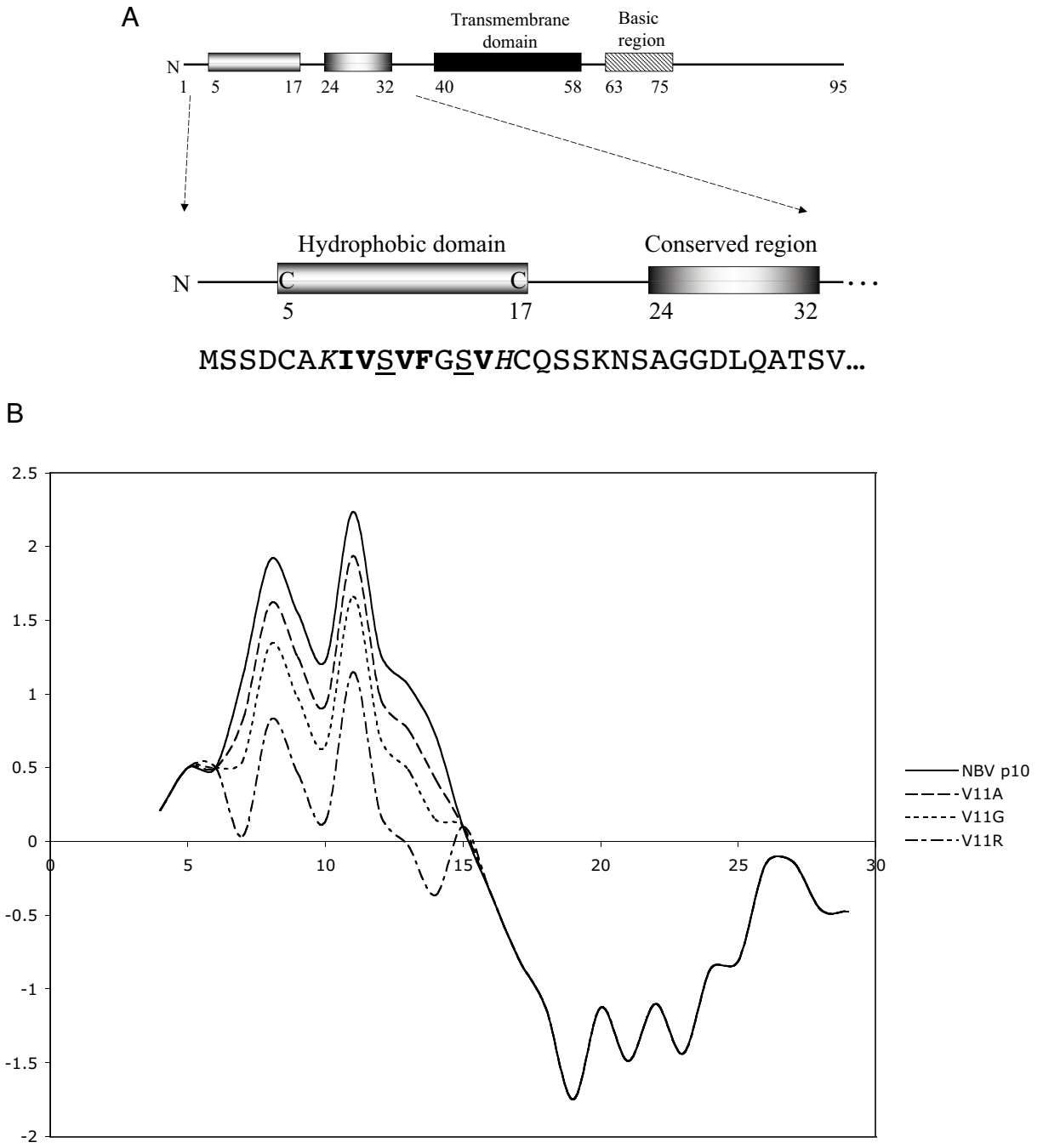

FIG. 1. Sequence and hydrophobicity plot of the HD of NBV p10 and its mutants. (A) Schematic representation of the NBV p10 protein and its ectodomain. The figure on top represents the complete NBV p10 protein, with the transmembrane domain and the basic region labeled. In the lower figure, the HD and the conserved region, so named because the region is highly conserved between NBV p10 and the p10 proteins of avian reoviruses, are shown with the corresponding amino acid sequence. Within the HD, hydrophobic residues are shown in boldface, hydrophilic residues are underlined, and charged residues are italicized. (B) Kyte-Doolittle plot of the first 32 N-terminal residues of native NBV p10, shown as a solid line, along with representative mutants V11A, V11G, and V11R.

V9L and V11L retained at least 50% of wild-type fusion activity. Position 12 showed no detectable fusion when substituted with Gly, Ala, Arg, or Tyr. However, when an aromatic (Trp) or highly hydrophobic residue (Leu) was introduced, the fusion extent remained at wild-type level. Overall, these results show that hydrophobic residues within the HD are important for fusion and that a highly hydrophobic residue at position 12 plays a crucial role in mediating fusion.

Syncytium formation by p10 mutants with point mutations at hydrophilic or charged residues. Unlike other known fusion peptides (36, 38), the HD of both NBV and ARV p10 contain interspersed hydrophilic residues. To explore the role of these

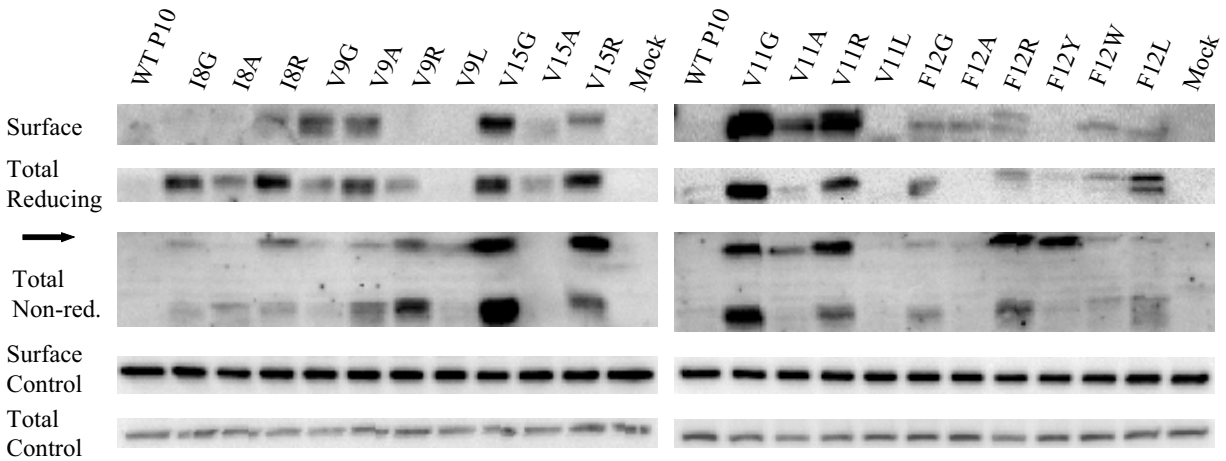

FIG. 2. Surface and total cell expression of NBV p10 proteins with mutations at hydrophobic residues. Gly, Ala, and Arg were introduced as point mutations at positions 8-Ile, 9-Val, 11-Val, 12-Phe, and 15-Val. In addition, Tyr and Trp were introduced at 12-Phe. Conservative mutations V9L and V11L were also constructed. A total of 0.75 μg of each plasmid encoding mutant p10 was transfected into confluent Vero cells in 12-well plates, with each well containing 5×10^5 cells. At 18 h posttransfection, Vero cells expressing mutant p10s were biotinylated, lysed, and analyzed by SDS–15% polyacrylamide gel electrophoresis under reducing (surface) or nonreducing (total cell lysate) conditions. Western blot analyses were performed to visualize the expression levels. Mock transfection with the pCAGGS vector without inserts served as a negative control. For internal control, the Western blot membranes were reprobed with anti-human transferrin receptor antibody. The standard deviations of the internal controls as quantitated by VersaDoc ranged from 12.8 to 17.9%. The mutants are labeled in the conventional way, e.g., V11R designates an arginine-for-valine substitution at position 11. The arrow indicates potential dimer formation. The data shown are representative of three separate experiments.

hydrophilic residues, we mutated 10-Ser and 14-Ser to Gly or Val. Mutations of 10-Ser and 14-Ser to Gly showed decreased fusion at early time points, with S14G showing a more pronounced decrease (Table 2). Mutations of these hydrophilic residues to Val showed even more pronounced decrease in fusion compared to the Gly mutants. However, the fusion extent increased over the observed time period: S10G and S10V reached wild-type level at 36 and 72 h posttransfection, respectively, while S14G and S14V reached 75% of the wild-type level at 72 h posttransfection. Substitution of the charged residue 16-His within the HD with Ala or Asp did not interfere with p10's fusion ability. These point mutations suggest that the Ser residues within the HD are important because of their hydrophilic nature. The role of the charged residues within the HD is less clear.

Lipid mixing and content mixing induced by NBV p10 mutants. To investigate whether fusion-negative p10 mutants were arrested at the hemifusion state (19, 32), where membrane lipids are mixed without the mixing of the content, we cocultured p10-transfected Vero cells with XC cells doubly labeled with R18 (lipid probe) and calcein (content probe). XC cells were chosen for their smaller size to facilitate distinction between the cell populations. Whereas the wild-type p10 showed extensive transfer of both dyes, fusion-negative mutants (I8G, V11G, V11R, F12G, F12A, F12R, F12Y, V15G, and V15R) showed no transfer of either dye (Fig. 5 and Fig. 6 [only representative mutants are shown]). These results indicated complete ablation of lipid mixing as well as content mixing.

DISCUSSION

Our studies (i) provided evidence that the HD functions as a fusion peptide, (ii) explored possible roles of the hydrophilic residues within the HD, and (iii) indicated that the overall hydrophobicity of the HD appears to be balanced for optimal expression and lipid membrane interaction.

Fusion peptides are known for their hydrophobic nature (13, 24). Presumably, the hydrophobic residues are required to associate with the target membrane and possibly to destabilize

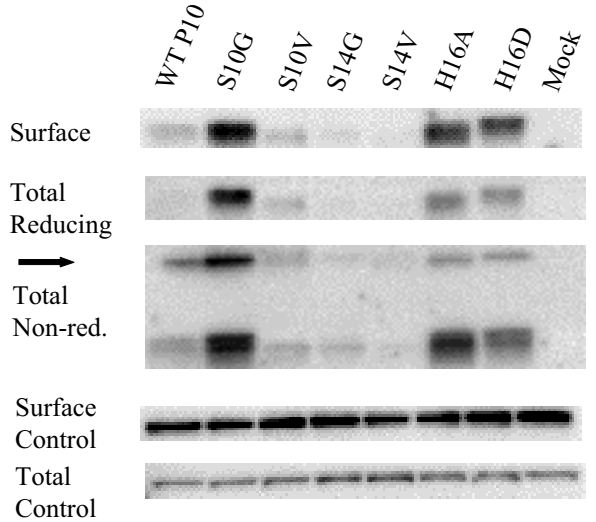

FIG. 3. Surface and total cell expression of NBV p10 proteins with mutations at hydrophilic or charged residues. Gly and Val were introduced at 10-Ser and 14-Ser. The charged residue 16-His was mutated to Ala and Asp. A total of 0.75 μg of each plasmid encoding mutant p10 protein was transfected into Vero cells, and expression levels were analyzed as described in Fig. 2. The standard deviations of the internal controls as quantitated by VersaDoc were 15.7 and 16.9% for the surface and total expressions, respectively. The arrow indicates potential dimer formation. The data shown are representative of three separate experiments.

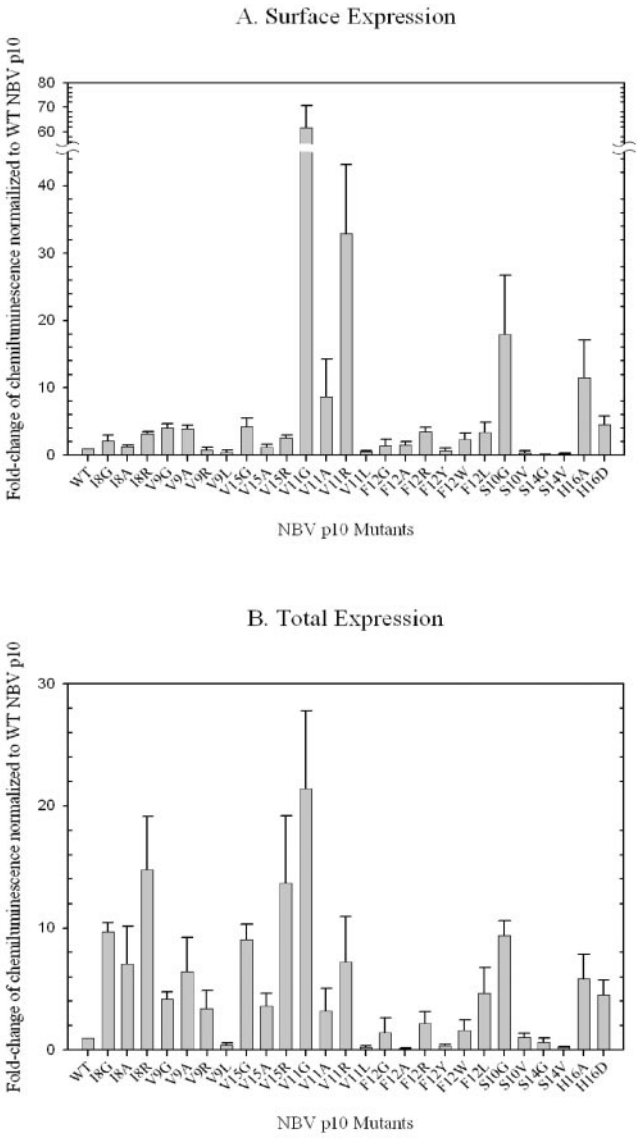

FIG. 4. Comparative analysis of surface (A) and total (B) expression levels of NBV p10 mutant proteins. Western blots of the NBV p10 protein and its mutants were exposed to the imaging system, VersaDoc, for quantitation of the chemiluminescent signals. The intensity of the signals for each mutant was normalized to that of the wild-type NBV p10 protein. The results shown are the average of three separate experiments, with the standard deviations indicated.

it as a first step in cell-cell fusion. There are a number of highly hydrophobic amino acids within the HD of NBV p10. In general, as we replaced each hydrophobic residue with amino acids of decreasing hydrophobicity, the extent of fusion decreased accordingly. Other studies (35) on the ARV p10 HD showed a similar general trend. In contrast, conservative changes did not significantly affect fusion. This result indicates that the hydrophobic residues within the HD contribute to membrane interactions analogous to those of fusion peptides in other viral fusion proteins. A recent study (35) provided molecular and biophysical analysis supporting the HD's candidacy as a fusion peptide. The Duncan group showed that synthetic peptides based on the HD of the ARV p10 protein mediated fusion of

TABLE 1. Syncytium formation over time by mutant NBV p10s with mutations at hydrophobic residues[a]

Construct	Syncytium formation[b] at:			
	24 h	36 h	48 h	72 h
NBV p10	++++	D	D	D
I8G	−	−	−	−
I8A	+++	++++	D	D
I8R	−	+	+	+
V9G	++	++	++	++
V9A	+++	+++	++++	D
V9R	−	−	+	+
V9L	+	++	++	+++
V11G	−	−	−	−
V11A	−	−	+	+
V11R	−	−	−	−
V11L	−	+++	++++	D
V15G	−	−	−	−
V15A	−	+++	++++	D
V15R	−	−	−	−
F12G	−	−	−	−
F12A	−	−	−	−
F12R	−	−	−	−
F12Y	−	−	−	−
F12W	+++	++++	D	D
F12L	+++	++++	D	D
Mock	−	−	−	−

[a] Gly, Ala, and Arg were introduced as point mutations at residues 8-Ile, 9-Val, 11-Val, 12-Phe, and 15-Val as described in Materials and Methods. In addition, Tyr and Trp were also introduced at 12-Phe. Conservative mutations V9L and V11L were also constructed.

[b] The extent of fusion induced by the mutant p10 protein was classified into either no fusion (−) or one of four levels of syncytium formation—+, 1 to 25%; ++, 26 to 50%; +++, 51 to 75%; and ++++, 76 to 100%—by comparison to the wild-type p10 protein. The extent of fusion induced by wild-type p10 was designated as "++++" (>80% of the surface area is covered by syncytial cells) at 24 h posttransfection. The result shown is representative of three separate experiments. D, detached.

liposomes. In the same study, they also showed that V15M and V19M mutations in HA-tagged ARV p10 protein inhibit fusion, whereas a T13M mutation retains the fusion ability. To further explore the role of hydrophobicity and charged residues within the HD, we performed an extensive mutagenesis study by mutating the residues to a range of amino acids with various degree of hydrophobicity.

In our mutational analysis, the presence of an aromatic or highly hydrophobic residue appeared to be essential at position

TABLE 2. Syncytium formation over time by mutant NBV p10s with mutations at hydrophilic or charged residues[a]

Construct	Syncytium formation[b] at:			
	24 h	36 h	48 h	72 h
NBV p10	++++	D	D	D
S10G	+++	++++	D	D
S10V	++	++	+++	++++
S14G	++	++	+++	+++
S14V	+	++	+++	+++
H16A	+++	++++	D	D
H16D	+++	++++	D	D
Mock	−	−	−	−

[a] Gly and Val were introduced at residues 10-Ser and 14-Ser. The charged residue 16-His was mutated to Ala or Asp as described in Materials and Methods.

[b] See Table 1, footnote *b*, for explanation of the results. The results shown are representative of three separate experiments.

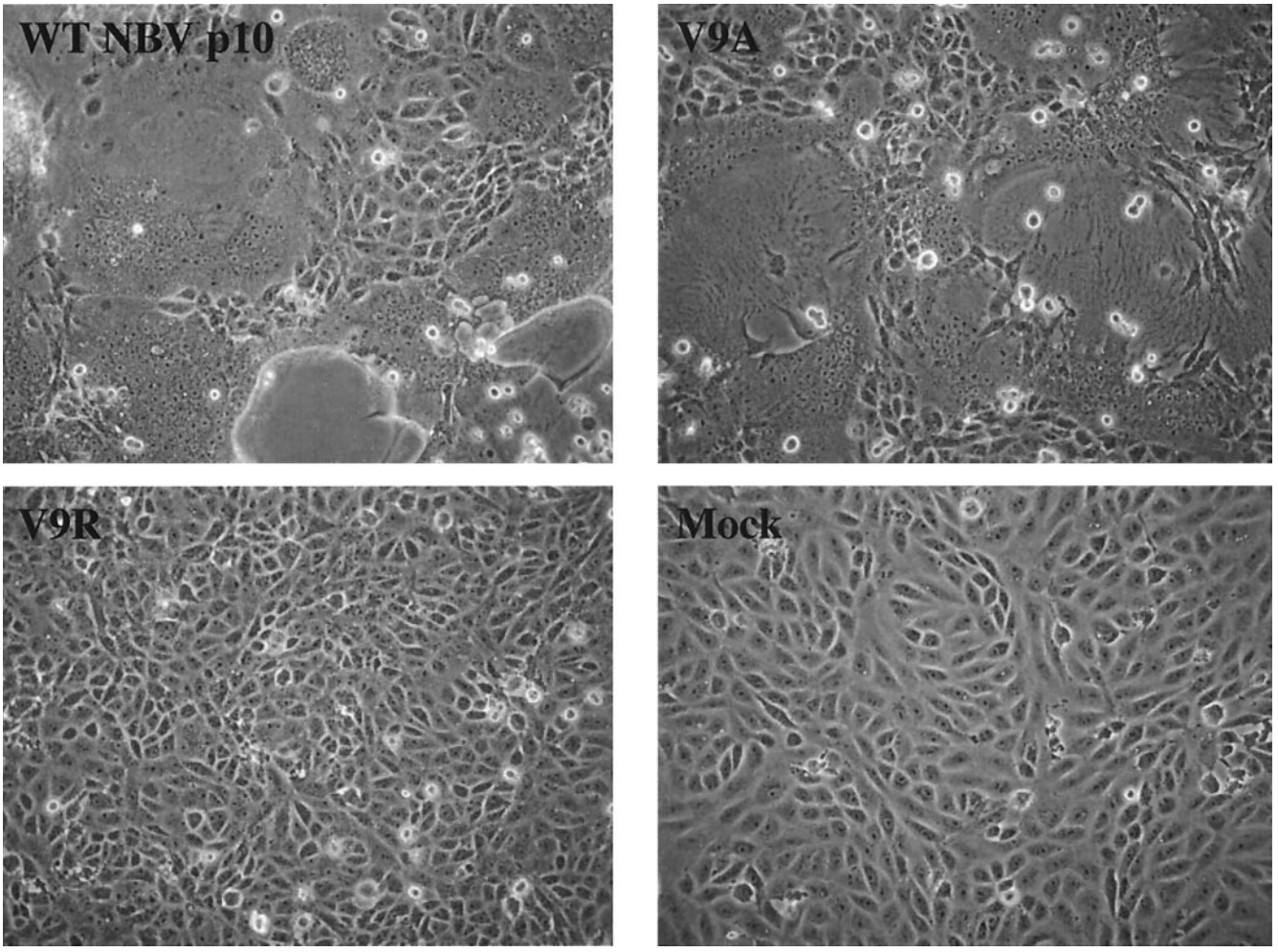

FIG. 5. Syncytium formation by NBV p10 and its mutants. Monolayers of Vero cells were transfected with pCAGGS expressing NBV p10 or its mutants. Mock-transfected cells served as negative control. At 24 h posttransfection, cells were photographed at ×190 magnification under an inverted light microscope. Only selected mutants are shown.

12 (31). The phenylalanine is positioned near the center of the HD and is followed immediately by the only glycine (which may provide flexibility in the peptide chain) within the HD. If the two cysteine residues flanking the HD mediate a fusion peptide loop formation, we speculate that the phenylalanine is the target-membrane-facing residue that initiates lipid mixing. Despite having a similar requirement for hydrophobic residues, there are some notable differences between the HD of NBV p10 and other fusion peptides or "fusion loops" such as that of the Ebola glycoprotein (9, 10, 17, 39): (i) the HD of NBV p10 has only 11 amino acids, whereas other fusion peptides have 16 to 18 residues, and (ii) the HD lacks interspersed glycine and alanine residues—only one of each residue is found. This suggests that the HD of p10 might function differently from other fusion peptides.

The presence of interspersed hydrophilic residues in the HD is a significant departure from known fusion peptides. Although hydrophilic residues can be found toward the C-terminal end of other fusion peptides like that of the influenza virus HA and paramyxovirus F glycoproteins, the hydrophilic residues of the NBV p10 HD are found in the middle of what would otherwise be the most hydrophobic stretch. When we replaced the serine residues with hydrophobic residues, we observed reduced surface expression of p10 and delayed syncytium formation. This result suggests that the HD might act as a degradation signal in the regulation of p10 expression (25, 26, 30). During normal transport to the cell surface, the fusion peptides of other viral glycoproteins are buried inside the molecules since the exposure of hydrophobic patches might activate the endoplasmic reticulum degradation machinery. The fact that increased hydrophobicity of the HD leads to a reduced surface steady-state level suggests that the NBV HD might be exposed during transport to the surface. If the HD is solvent exposed when we increased the hydrophobicity through serine-to-valine substitution, we would anticipate more rapid degradation of the mutant p10 proteins, leading to a reduced steady state and delayed onset of fusion. This hypothesis is also supported by our results showing that when hydrophobic residues were mutated to less hydrophobic or charged residues, the steady-state levels, both on the cell surface and overall, were much elevated compared to the wild type (even though these mutants can no longer cause fusion). Our mutational

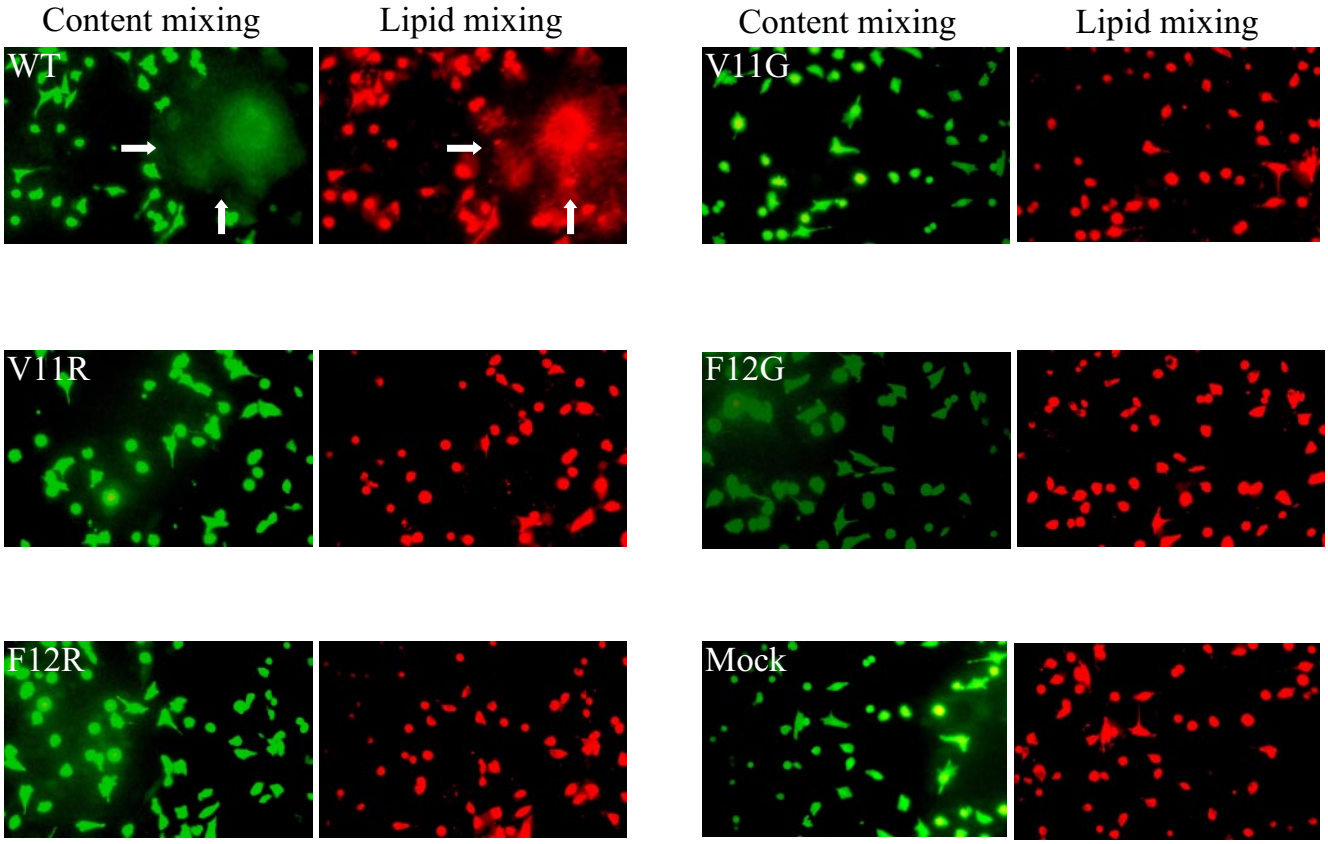

FIG. 6. Lipid mixing and content mixing by NBV p10 mutants. Vero cells expressing the fusion-negative mutants I8G, V11G, V11R, F12G, F12A, F12R, F12Y, V15G, and V15R were suspended and reseeded with XC cells doubly labeled with R18 (for lipid mixing [red color]) and Calcein AM (for content mixing [green color]). Wild-type p10 and mock transfection are shown as controls. The experiment was repeated once. Only selected mutants are shown since none of the fusion-negative mutants caused lipid mixing. The white arrows in the wild-type panels outline a syncytium.

analysis thus reveals an interesting theme that the HD strikes a balance between the need for hydrophobic residues for fusion and the need for hydrophilic residues for expression in sufficient quantities at the cell surface.

The structural features of NBV p10 pose numerous questions as we attempt to delineate its fusion mechanism. When class I fusion proteins are compared to p10, we find significant incongruence. The ectodomain of NBV p10 lacks heptad repeat regions, thus extension and refolding of the molecule as occurs with class I fusion protein is unlikely. The intervening region of 18 residues between the HD and the transmembrane domain of p10 could potentially function as a hinge region analogously to the loop region found between the two sets of heptad repeats of class I fusion proteins (21). However, because of the simple structure of p10, it is uncertain that p10 can derive the activation energy required for refolding (27). A triggering event such as receptor binding or pH change is also probably unnecessary since p10 causes fusion at neutral pH in a range of cell types (unpublished observation). An alternative model of the fusion mechanism includes the involvement of cellular components. It is also possible that p10 acts like a detergent that simply destabilizes lipid membranes (4). Further study of the structures of p10 and other FAST proteins may provide clues to the fusion mechanism.

ACKNOWLEDGMENTS

This study was supported by grant AI054337 from the National Institutes of Health.

We thank Tanya Cassingham for assistance in manuscript preparation and David Steinhauer (Emory University) for helpful suggestions.

REFERENCES

1. **Agutter, P. S., P. C. Malone, and D. N. Wheatley.** 1995. Intracellular transport mechanisms: a critique of diffusion theory. J. Theor. Biol. **176:**261–272.
2. **Bagai, S., and R. A. Lamb.** 1995. Quantitative measurement of paramyxovirus fusion: differences in requirements of glycoproteins between simian virus 5 and human parainfluenza virus 3 or Newcastle disease virus. J. Virol. **69:** 6712–6719.
3. **Blobel, C. P., T. G. Wolfsberg, C. W. Turck, D. G. Myles, P. Primakoff, and J. M. White.** 1992. A potential fusion peptide and an integrin ligand domain in a protein active in sperm-egg fusion. Nature **356:**248–252.
4. **Bonnafous, P., and T. Stegmann.** 2000. Membrane perturbation and fusion pore formation in influenza hemagglutinin-mediated membrane fusion: a new model for fusion. J. Biol. Chem. **275:**6160–6166.
5. **Carr, C. M., C. Chaudhry, and P. S. Kim.** 1997. Influenza hemagglutinin is spring-loaded by a metastable native conformation. Proc. Natl. Acad. Sci. USA **94:**14306–14313.
6. **Corcoran, J. A., and R. Duncan.** 2004. Reptilian reovirus utilizes a small type III protein with an external myristylated amino terminus to mediate cell-cell fusion. J. Virol. **78:**4342–4351.
7. **Cross, K. J., S. A. Wharton, J. J. Skehel, D. C. Wiley, and D. A. Steinhauer.** 2001. Studies on influenza haemagglutinin fusion peptide mutants generated by reverse genetics. EMBO J. **20:**4432–4442.
8. **Dawe, S., J. Boutilier, and R. Duncan.** 2002. Identification and characterization of a baboon reovirus-specific nonstructural protein encoded by the bicistronic s4 genome segment. Virology **304:**44–52.

9. **Delos, S. E., J. M. Gilbert, and J. M. White.** 2000. The central proline of an internal viral fusion peptide serves two important roles. J. Virol. **74:**1686–1693.
10. **Delos, S. E., and J. M. White.** 2000. Critical role for the cysteines flanking the internal fusion peptide of avian sarcoma/leukosis virus envelope glycoprotein. J. Virol. **74:**9738–9741.
11. **Duncan, R., Z. Chen, S. Walsh, and S. Wu.** 1996. Avian reovirus-induced syncytium formation is independent of infectious progeny virus production and enhances the rate, but is not essential, for virus-induced cytopathology and virus egress. Virology **224:**453–464.
12. **Duncan, R., and K. Sullivan.** 1998. Characterization of two avian reoviruses that exhibit strain-specific quantitative differences in their syncytium-inducing and pathogenic capabilities. Virology **250:**263–272.
13. **Durell, S. R., I. Martin, J. M. Ruysschaert, Y. Shai, and R. Blumenthal.** 1997. What studies of fusion peptides tell us about viral envelope glycoprotein-mediated membrane fusion. Mol. Membr. Biol. **14:**97–112.
14. **Gard, G., and R. W. Compans.** 1970. Structure and cytopathic effects of Nelson Bay virus. J. Virol. **6:**100–106.
15. **Gibbons, D. L., A. Ahn, M. Liao, L. Hammar, R. H. Cheng, and M. Kielian.** 2004. Multistep regulation of membrane insertion of the fusion peptide of Semliki Forest virus. J. Virol. **78:**3312–3318.
16. **Gibbons, D. L., I. Erk, B. Reilly, J. Navaza, M. Kielian, F. A. Rey, and J. Lepault.** 2003. Visualization of the target-membrane-inserted fusion protein of Semliki Forest virus by combined electron microscopy and crystallography. Cell **114:**573–583.
17. **Glombik, M. M., A. Kromer, T. Salm, W. B. Huttner, and H. H. Gerdes.** 1999. The disulfide-bonded loop of chromogranin B mediates membrane binding and directs sorting from the trans-Golgi network to secretory granules. EMBO J. **18:**1059–1070.
18. **Jahn, R., T. Lang, and T. C. Sudhof.** 2003. Membrane fusion. Cell **112:**519–533.
19. **Kemble, G. W., T. Danieli, and J. M. White.** 1994. Lipid-anchored influenza hemagglutinin promotes hemifusion, not complete fusion. Cell **76:**383–391.
20. **Kielian, M.** 1995. Membrane fusion and the alphavirus life cycle. Adv. Virus Res. **45:**113–151.
21. **Kozlov, M. M., and L. V. Chernomordik.** 1998. A mechanism of protein-mediated fusion: coupling between refolding of the influenza hemagglutinin and lipid rearrangements. Biophys. J. **75:**1384–1396.
22. **Kyte, J., and R. F. Doolittle.** 1982. A simple method for displaying the hydropathic character of a protein. J. Mol. Biol. **157:**105–132.
23. **Liu, H. J., L. H. Lee, H. W. Hsu, L. C. Kuo, and M. H. Liao.** 2003. Molecular evolution of avian reovirus: evidence for genetic diversity and reassortment of the S-class genome segments and multiple cocirculating lineages. Virology **314:**336–349.
24. **Luneberg, J., I. Martin, F. Nussler, J. M. Ruysschaert, and A. Herrmann.** 1995. Structure and topology of the influenza virus fusion peptide in lipid bilayers. J. Biol. Chem. **270:**27606–27614.
25. **Matlack, K. E., W. Mothes, and T. A. Rapoport.** 1998. Protein translocation: tunnel vision. Cell **92:**381–390.
26. **McCracken, A. A., and J. L. Brodsky.** 2003. Evolving questions and paradigm shifts in endoplasmic-reticulum-associated degradation (ERAD). Bioessays **25:**868–877.
27. **Melikyan, G. B., R. M. Markosyan, H. Hemmati, M. K. Delmedico, D. M. Lambert, and F. S. Cohen.** 2000. Evidence that the transition of HIV-1 gp41 into a six-helix bundle, not the bundle configuration, induces membrane fusion. J. Cell Biol. **151:**413–423.
28. **Ni, Y., and R. F. Ramig.** 1993. Characterization of avian reovirus-induced cell fusion: the role of viral structural proteins. Virology **194:**705–714.
29. **Niwa, H., K. Yamamura, and J. Miyazaki.** 1991. Efficient selection for high-expression transfectants with a novel eukaryotic vector. Gene **108:**193–199.
30. **Plemper, R. K., S. Bohmler, J. Bordallo, T. Sommer, and D. H. Wolf.** 1997. Mutant analysis links the translocon and BiP to retrograde protein transport for ER degradation. Nature **388:**891–895.
31. **Pritsker, M., J. Rucker, T. L. Hoffman, R. W. Doms, and Y. Shai.** 1999. Effect of nonpolar substitutions of the conserved Phe11 in the fusion peptide of HIV-1 gp41 on its function, structure, and organization in membranes. Biochemistry **38:**11359–11371.
32. **Qiao, H., R. T. Armstrong, G. B. Melikyan, F. S. Cohen, and J. M. White.** 1999. A specific point mutant at position 1 of the influenza hemagglutinin fusion peptide displays a hemifusion phenotype. Mol. Biol. Cell **10:**2759–2769.
33. **Rey, F. A., F. X. Heinz, C. Mandl, C. Kunz, and S. C. Harrison.** 1995. The envelope glycoprotein from tick-borne encephalitis virus at 2 Å resolution. Nature **375:**291–298.
34. **Shmulevitz, M., and R. Duncan.** 2000. A new class of fusion-associated small transmembrane (FAST) proteins encoded by the non-enveloped fusogenic reoviruses. EMBO J. **19:**902–912.
35. **Shmulevitz, M., R. F. Epand, R. M. Epand, and R. Duncan.** 2004. Structural and functional properties of an unusual internal fusion peptide in a nonenveloped virus membrane fusion protein. J. Virol. **78:**2808–2818.
36. **Skehel, J. J., K. Cross, D. Steinhauer, and D. C. Wiley.** 2001. Influenza fusion peptides. Biochem. Soc. Trans. **29:**623–626.
37. **Skehel, J. J., and D. C. Wiley.** 2000. Receptor binding and membrane fusion in virus entry: the influenza hemagglutinin. Annu. Rev. Biochem. **69:**531–569.
38. **Steinhauer, D. A., S. A. Wharton, J. J. Skehel, and D. C. Wiley.** 1995. Studies of the membrane fusion activities of fusion peptide mutants of influenza virus hemagglutinin. J. Virol. **69:**6643–6651.
39. **Weissenhorn, W., A. Carfi, K. H. Lee, J. J. Skehel, and D. C. Wiley.** 1998. Crystal structure of the Ebola virus membrane fusion subunit, GP2, from the envelope glycoprotein ectodomain. Mol. Cell **2:**605–616.
40. **White, J. M.** 1990. Viral and cellular membrane fusion proteins. Annu. Rev. Physiol. **52:**675–697.
41. **Wilson, I. A., J. J. Skehel, and D. C. Wiley.** 1981. Structure of the haemagglutinin membrane glycoprotein of influenza virus at 3 Å resolution. Nature **289:**366–373.